Discovery Decomposition

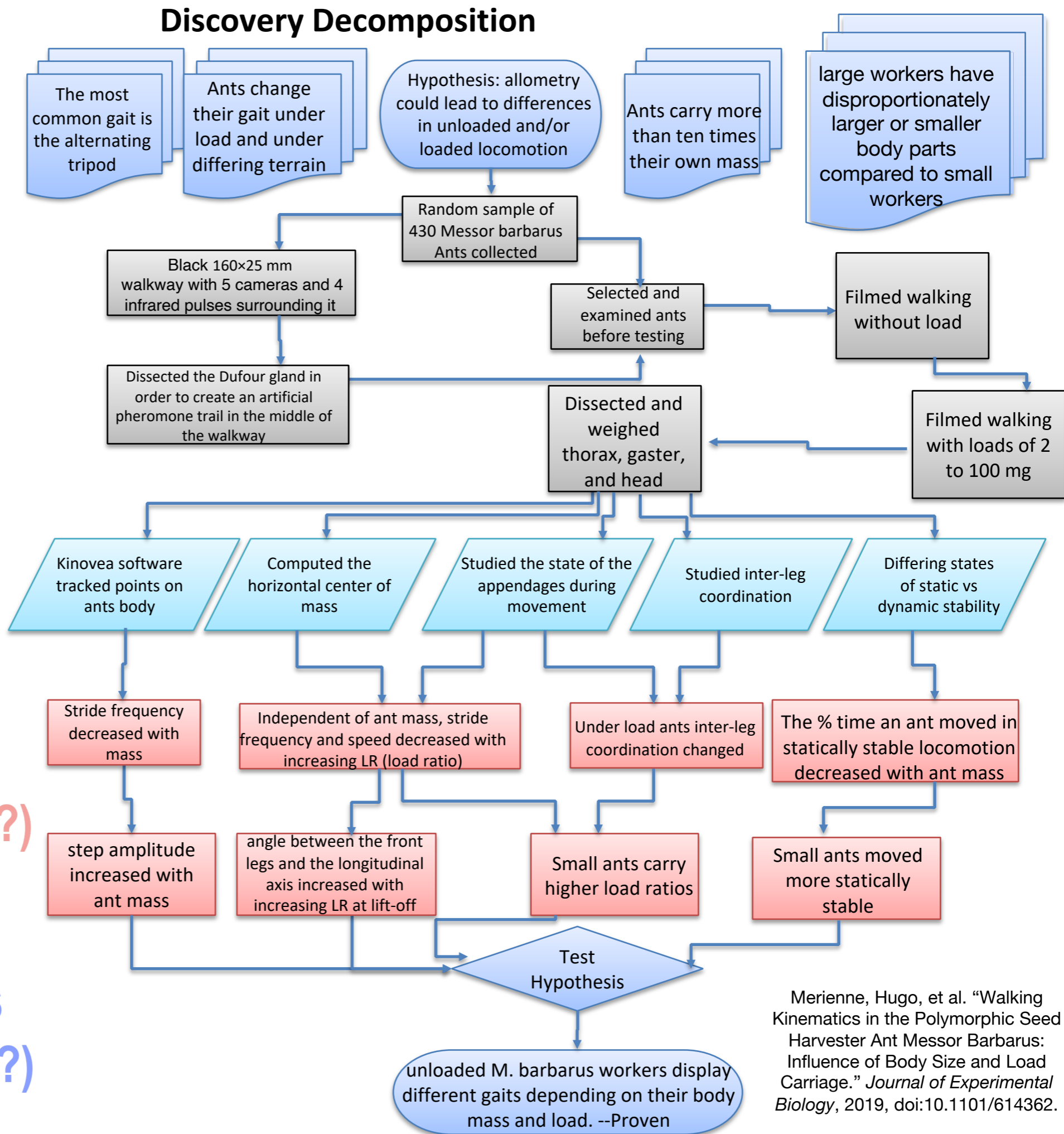**Background & Hypothesis (What was known?)**

- The most common gait is the alternating tripod
- Ants change their gait under load and under differing terrain
- Hypothesis: allometry could lead to differences in unloaded and/or loaded locomotion
- Ants carry more than ten times their own mass
- large workers have disproportionately larger or smaller body parts compared to small workers

Methods (What was done?)

- Random sample of 430 Messor barbarus Ants collected
- Black 160×25 mm walkway with 5 cameras and 4 infrared pulses surrounding it
- Selected and examined ants before testing
- Filmed walking without load
- Dissected the Dufour gland in order to create an artificial pheromone trail in the middle of the walkway
- Dissected and weighed thorax, gaster, and head
- Filmed walking with loads of 2 to 100 mg

Results (What was measured?)

- Kinovea software tracked points on ants body
- Computed the horizontal center of mass
- Studied the state of the appendages during movement
- Studied inter-leg coordination
- Differing states of static vs dynamic stability

Conclusions (What was discovered?)

- Stride frequency decreased with mass
- Independent of ant mass, stride frequency and speed decreased with increasing LR (load ratio)
- Under load ants inter-leg coordination changed
- The % time an ant moved in statically stable locomotion decreased with ant mass
- step amplitude increased with ant mass
- angle between the front legs and the longitudinal axis increased with increasing LR at lift-off
- Small ants carry higher load ratios
- Small ants moved more statically stable

Test Hypothesis (What is now known?)

- Test Hypothesis
- unloaded M. barbarus workers display different gaits depending on their body mass and load. --Proven

Merienne, Hugo, et al. "Walking Kinematics in the Polymorphic Seed Harvester Ant Messor Barbarus: Influence of Body Size and Load Carriage." *Journal of Experimental Biology*, 2019, doi:10.1101/614362.

Design Solution	Analogy Check	Design Problem
Ant Kinematics		**Death defiANT (ant rescue robot)**
Function (What does system or organism do?)		**Function** (What do you want system to do?)
Carry ten times more than their mass	Similar	Lift relatively heavy loads of differing shapes
	N/A	Rescue people from fallen buildings / cave-ins
Structural Components (What is structure or organization of system?)		**Structural Components** (What can the structure be?)
Differing structure based on size of ant	Uncertain	metal and polymer
6 Ant legs	Similar	6 robot legs
Operating Environment (Where?)		**Operating Environment** (Where?)
Dirt / differing terrain both inside and outside	Similar	Differing terrains
	N/A	Fallen buildings / rock / caves
Size (What is size?)		**Size** (What size needed?)
A couple millimeters	Uncertain	2 feet
Mechanisms (How does system work?)		**Mechanisms** (How do you want the system to work?)
Changes the center of mass to carry more and stay stable	Similar	Change center of mass to carry more and stay stable
Digs in with hind legs to carry more weight	Similar	Dig in with back legs to support more weight
Change inter-leg coordination to carry more	Similar	Change leg movements to support more weight
Characteristics/Specification (Which are distinguishing?)		**Characteristics/Specification** (What are your specifications?)
Uses a tripod gait that changes with load size	Similar	Change gait, center of mass, and legs to supporter more weight
Relatively small bodies	N/A	Be able to pick up rocks
Performance Criteria (How well does system work?)		**Performance Criteria** (How well must the system work?)
100% of the time	Similar	100% of the time
Constraints (What compromises system?)		**Constraints** (Can compromises be removed?)
It grows into full size	N/A	Manufactured at full size
Even fully grown ants at relatively small	N/As	Increase size during manufacturing

The Company of Biologists

RESEARCH ARTICLE

Walking kinematics in the polymorphic seed harvester ant *Messor barbarus*: influence of body size and load carriage

Hugo Merienne, Gérard Latil, Pierre Moretto and Vincent Fourcassié*

ABSTRACT

Ants are famous in the animal kingdom for their amazing load-carrying performance. Yet, the mechanisms that allow these insects to maintain their stability when carrying heavy loads have been poorly investigated. Here, we present a study of the kinematics of unloaded and loaded locomotion in the polymorphic seed-harvesting ant *Messor barbarus*. In this species, large ants have larger heads relative to their size than small ants. Hence, their center of mass is shifted forward, and even more so when they are carrying a load in their mandibles. We tested the hypothesis that this could lead to large ants being less statically stable than small ants, thus explaining their lower load-carrying ability. We found that large ants were indeed less statically stable than small ants when walking unloaded, but they were nonetheless able to adjust their stepping pattern to partly compensate for this instability. When ants were walking loaded on the other hand, there was no evidence of different locomotor behaviors in individuals of different sizes. Loaded ants, whatever their size, move too slowly to maintain their balance through dynamic stability. Rather, they seem to do so by clinging to the ground with their hind legs during part of a stride. We show through a straightforward model that allometric relationships have a minor role in explaining the differences in load-carrying ability between large ants and small ants, and that a simple scale effect is sufficient to explain these differences.

KEY WORDS: Biomechanics, Kinematics, Locomotion, Load transport, Ants, Allometry

INTRODUCTION

The locomotion of animals can be described as a succession of strides that follows a specific inter-leg coordination pattern called gait (Alexander, 2003). In hexapod animals such as insects the most common gait is the alternating tripod (Delcomyn, 1981), in which the animal walks by alternating the movement of two distinct sets of legs (the ipsilateral front and hind leg and the contralateral mid leg, e.g. L1, L3, R2 and R1, R3, L2, respectively, with L for left and R for right), each of which forms a tripod supporting the body. In its ideal form, the two tripods perfectly alternate: all the legs in one tripod group simultaneously lift-off while all the legs of the other tripod group are still on the ground. However, depending on various features of their locomotion, insects can also adopt more complex gait. For example, the pattern of leg coordination can change with locomotory speed (Bender et al., 2011; Wosnitza et al., 2013;

Mendes et al., 2013; Wahl et al., 2015), walking curvature (Zollikofer, 1994a) and forwards or backwards movement (Pfeffer et al., 2016). Insects also adapt their gait according to the features of the terrain on which they are moving, for example when they walk on a non-level substrate (Seidl and Wehner, 2008; Reinhardt et al., 2009; Grabowska et al., 2012; Ramdya et al., 2017; Wöhrl et al., 2017) or when they climb over obstacles (Watson et al., 2002). Another factor that is known to have an effect on leg coordination during locomotion in terrestrial vertebrates (Jagnandan and Higham, 2018) but that has been less well studied in insects is the change in the total mass an individual has to put in motion. Changes in total mass can be progressive or sudden and can occur in a variety of situations: in female insects during egg development and after oviposition, during autotomy (the voluntary shedding of a body segment; Fleming and Bateman, 2007; Lagos, 2017) or, in the most common case, when insects are transporting food, either internally, after ingesting liquid, or externally, in their mandibles. In all these situations, the change in total mass induces a shift in the center of mass of the insect, which can profoundly affect its locomotion.

Ants offer a very good model to study the effect of changes in total mass on walking kinematics for four reasons. First, they are notorious for their load-carrying ability and can routinely transport loads (prey items, seeds, nest material, nestmates and brood) weighing more than ten times their own mass over tens of meters (Bernadou et al., 2016). When an item is too heavy be carried alone, ants can also walk backward to their nest and drag it (Bernadou et al., 2016), or they can perform collective load transport (Czaczkes and Ratnieks, 2013). Second, the food collected by ants can be transported internally or externally. The shift in their center of mass can thus vary both in intensity and direction, which is likely to disrupt their walking kinematics in different ways and makes ants an interesting biological model for the study of the biomechanics of load transport. Third, as a result of the high number of species in their taxon (Hölldobler and Wilson, 1990), the size and shape of ant bodies is extremely variable, which probably affects the kinematics of their locomotion differently. And fourth, ants live in very diverse environments and can be subterranean, ground-living or arboreal (Hölldobler and Wilson, 1990), which is bound to constrain their movements and affect their locomotion (Gravish et al., 2013; Seidl and Wehner, 2008; Reinhardt et al., 2009; Wöhrl et al., 2017).

The effects of changes in total mass due to load carriage on the walking kinematics of ants have been poorly explored in the ant literature. The main effect of carrying a load in the mandibles is to induce a forward shift of the center of mass of the system formed by the ant and the load they carry. However, according to Hughes (1952), insects could counter this effect and achieve balanced locomotion by using static stability, i.e. by keeping the projection of their center of mass on the horizontal plane within the polygon formed by the legs simultaneously in contact with the ground (called the polygon of support). In fact, this is what loaded ants do. For example, *Cataglyphis fortis* workers ensure static stability by

placing their front legs in a more forward position when loaded than when unloaded and by reducing their stride length (Zollikofer, 1994b). In *Atta vollenweideri*, whose foraging workers carry elongated pieces of grass over their head, ants increase their mechanical stability by increasing the number of legs simultaneously in contact with the ground. They do so by increasing over consecutive steps the overlap between the stance (retraction) phase of the supporting tripod and some of the legs of the other tripod (mostly the front leg) and by dragging their hind legs during the swing (protraction) phase (Moll et al., 2013). These ants also adjust the angle of the load they carry so that the projection of their center of mass on the horizontal plane remains within the polygon of support (Moll et al., 2013).

In this paper, we studied the effect of load carriage on the walking kinematics of the seed-harvesting ant *Messor barbarus*, an ant species that is characterized by a highly polymorphic worker caste, i.e. a high variability in the size of individuals within the same colony. In addition, this polymorphism is characterized by allometric relationships between the different parts of the body (Bernadou et al., 2016), which means that large workers are not an enlarged copy of small workers but that some of their body parts are disproportionately larger or smaller than those of small workers (Bonner, 2006). In fact, relative to their mass, their legs are shorter and their head larger than those of small workers. Here, we hypothesized that this allometry could lead to differences in unloaded and/or loaded locomotion in different-sized workers and thus could explain the differences observed in their load-carrying ability (Bernadou et al., 2016). To test this, we ran an experiment in which we compared the kinematics of workers tested first unloaded and then carrying loads whose relative mass we varied in a systematic way across different-sized ants.

MATERIALS AND METHODS
Study species and rearing conditions
We used workers from a large colony (∼5000 individuals) of *Messor barbarus* (Linnaeus 1767) collected in April 2018 at St Hippolyte (Pyrénées Orientales) on the French Mediterranean coast. *Messor barbarus* is a seed harvester ant whose mature colonies can shelter several tens of thousands of individuals (Cerdan, 1989). Its workers display a polymorphism characterized by a continuous monophasic allometry between head mass and thorax length (Heredia and Detrain, 2000; Bernadou et al., 2016). For the sake of clarity, we will refer in this study to the (mesosoma+petiole) part of the ants as the 'thorax', even if in ants it contains some segments of the abdomen. Individuals in the colony ranged from 1.5 to 40 mg in mass (mean±s.d. for a random sample of 430 workers: 6.9± 5.1 mg) and from 2 to 15 mm in length. The whole colony was kept in a box (L×W×H: 50×30×15 cm) with Fluon®-coated walls to prevent ants from escaping. Ants nested inside test tubes (length: 20 cm; diameter: 2.5 cm) covered with opaque paper. They had access to water *ad libitum* and to seeds of various species (canary grass, niger, oats). The experimental room was kept at a constant temperature of 28°C and under a 12 h:12 h light:dark regime.

Experimental setup
The setup we used in our experiment was designed and built by a private company (R&D Vision, France. http://www.rd-vision.com). It consisted of a walkway (160×25 mm) covered with a piece of black paper (Canson® Mi-Teintes®, fine grain side, 160 g m⁻²) on which the ants walked during the experiment. The walkway was surrounded by five synchronized high-speed video cameras (JAI GO-5000M-PMCL: frequency: 250 Hz; resolution: 30 μm pixel⁻¹

for the top camera, 20 μm pixel⁻¹ for the others), one placed above the walkway and four placed on its sides (Fig. 1). Four infrared strobe spots (λ=850 nm; pulse frequency: 250 Hz), synchronized with the cameras, were used to illuminate the walkway from above, allowing a better contrast between the ants and the background on the videos. The temperature on the walkway was monitored with an infrared thermometer (MS pro, Optris, USA, http://www.optris.com). Over the course of the experiment the temperature was 28± 1.4°C (mean±s.d.).

Experimental protocol
All experiments were performed between April and July 2018. On the first day of a week in which we tested ants, we installed a bridge between the colony and a box in which a few seeds were placed. We then collected one ant out of three in 1 h that carried a seed back to the colony. These ants were kept apart and used for the experiment over the following days. We also collected a few ants (weighing between 10 and 15 mg) to dissect their Dufour gland in order to create an artificial pheromone trail in the middle of the walkway (Heredia and Detrain, 2000). Since ants tended to follow the trail, this increased the chance of obtaining a straighter path in the middle of the walkway, which allowed us to neglect the effect of path curvature on ant kinematics (Zollikofer, 1994a). In order to extract the Dufour gland, ants were first anesthetized by placing them in a vial plunged in crushed ice, then killed by removing their head and fixed on their back with insect pins under a binocular microscope. Their gaster was opened transversally with a scalpel following the first sternite and the ventral part was pulled away. The poison gland and the fat gland were then gently removed until the Dufour gland became visible. This latter was then collected and placed in a hexane solution to extract the trail pheromone. We used a concentration of 1 gland per 20 μl, which has been shown to be sufficient to elicit a clear trail-following response in *M. barbarus* workers (Heredia and Detrain, 2000).

Each time an ant was tested, it was picked from the group of ants that had been separated on the first day of the week, then weighed and isolated in a small box with access to water. The ant was first tested unloaded and then loaded with lead fishing weights whose mass ranged from 2 to 100 mg. The ant and its load were chosen in order to cover the range of ant mass found in our colony and a range of load ratio [defined as: 1+(load mass/ant mass), see Bartholomew et al., 1988] between 1.2 and 7, corresponding to that of most of the items spontaneously seized and carried by *M. barbarus* workers in the field (Bernadou et al., 2016).
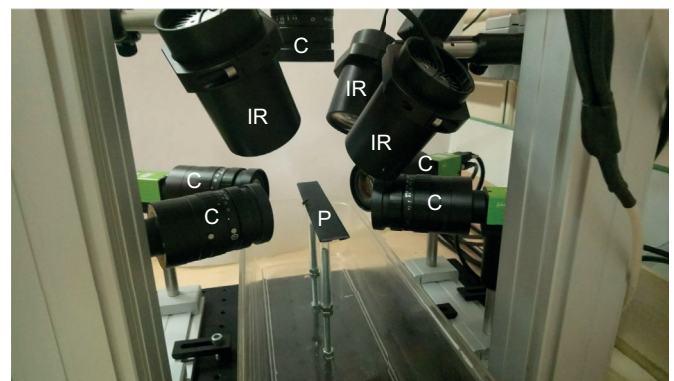

Fig. 1. Setup of the video acquisition system. C, cameras; IR, infra-red spots; P, 25 mm wide walkway.

After every fifth ant tested, we made an artificial trail on the walkway by depositing a 1 µl droplet of the Dufour gland extract with a 10 µl syringe at 1 cm intervals. To reduce stress, ants were transferred from their individual boxes to the walkway by letting them climb up and down on a pencil. Once on the walkway, the movement of the ant was recorded as soon as it started to walk along a more or less straight path. The ant was then captured at the end of the walkway and anesthetized by placing it in a vial plunged in crushed ice. It was then fixed dorsally with Plasticine under a binocular microscope with its head maintained horizontally. This allowed us to put a drop of superglue (Loctite, http://www.loctite.fr) on the top of its mandibles and to attach a fishing weight. The same procedure as for unloaded ants was then used to film loaded ants. At the end of the experiment, the ant was killed and we weighed its head, thorax (with the legs) and gaster separately to the nearest 0.1 mg with a precision balance (NewClassic MS semi-micro, Mettler, Toledo, USA). Whether unloaded or loaded, we filmed all ants for at least three strides. We defined a stride period as the time elapsed between two consecutive lift-offs of the right mid leg. For our analysis, we cropped the videos to a whole number of strides.

Data extraction and analysis

When several video recordings of the same ant had been made, we selected the videos (top view and one of the four side views) in which the ant had the straighter path. As a criteria for path straightness, we calculated the ratio of the distance actually traveled by ants (based on the horizontal trajectory of their center of mass) on the straight line distance between the first and last point of their trajectory and considered that the path was sufficiently straight when this ratio was lower than 1.2.

Several points were tracked with the software Kinovea (v. 0.8.15, https://www.kinovea.org) on the selected videos. On the top view, the (X,Y) coordinates of the following points were determined on each video frame (Fig. 2A–C): the extremity of the mandibles, the

neck, the junction between the petiole and the gaster, the extremity of the gaster and the position of the leg tarsus during the stance phases. In addition, we tracked the extremity of the load carried by loaded ants. The side view (Fig. 2B–D) was used to determine the state of each leg during locomotion (i.e. in stance phase, swung or dragged). Assuming a homogeneous distribution of the mass within each body parts, we then computed for each frame the approximate (x,y) position of the CoM of the three main body parts (plus the load) as the mean of the (x,y) coordinates of the points located at their two extremities. Finally, we computed the horizontal position of the center of mass (CoM) of the ants on each video frame as the barycenter of the CoM of their head, thorax and gaster weighed by their respective mass. In addition, we used these tracked points in order to compute the length of the main body parts of the ants on each frame. The length of their main body parts was then computed as the average length over all frames of a video.

For each video frame, we visually determined the state of each leg during locomotion (i.e. in stance phase, swung or dragged) on the side view of the ant and recorded the spatial position of the leg tarsus during the stance phases on the top view. These positions were expressed in a Cartesian coordinate system centered on the petiole of the ant, with the x-axis corresponding to the longitudinal axis of its body and the y-axis to the transverse axis (Fig. 2). In order to compare ants of different sizes, all distances were normalized to the body length of the ant (calculated from the tip of the gaster to the tip of the mandibles).

We computed the duty factor for each leg as the fraction of the stride that the leg was in contact with the ground (Ting et al., 1994; Spence et al., 2010). For each leg, we also computed the mean position of the tarsus end at lift-off (posterior extreme position, PEP) and at touch-down (anterior extreme position, AEP) by averaging the positions of the tarsus end over the strides we filmed. Since the path followed by ants was straight, we averaged the values of the right and left leg of each pair of legs when computing the duty
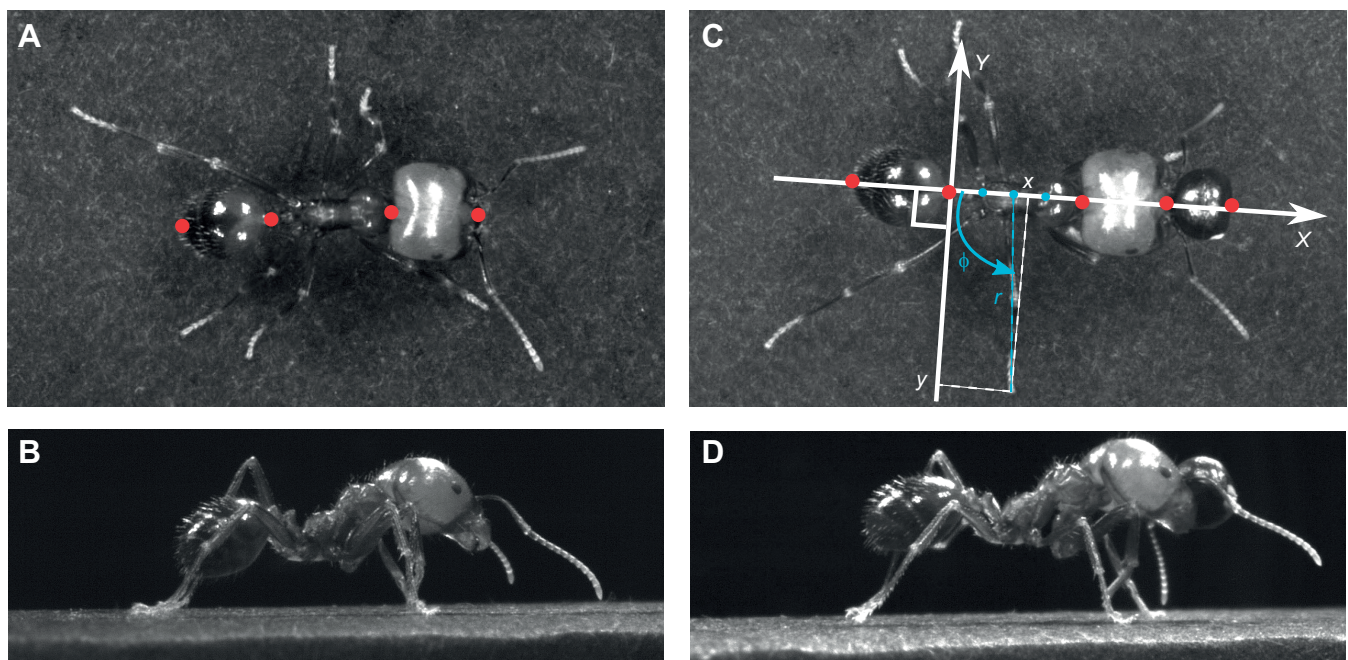

Fig. 2. Location of the points tracked on each ant. The snapshots show a top view (A,C) and a side view (B,D) of the same ant (ant mass=32.5 mg) tested in unloaded (A,B) and loaded condition (C,D) (load mass=63 mg). In C, the X-axis corresponds to the longitudinal body axis while the Y-axis corresponds to the transverse body axis. The position of the track points are represented in red. The blue points correspond to three equidistant points used as origin for the polar coordinate system of the three pairs of legs. As an example, the polar coordinates of the right mid leg (r,ϕ) are shown in C.

factors and leg positions. We expressed these mean positions at lift-off and touch-down in a polar coordinate system. As we did not track the positions of the leg coxae, we computed three virtual points at equidistant intervals between the neck and petiole and used them as origins for the polar coordinate system associated with the three pairs of legs. For all legs, we then computed the polar coordinates (r,ϕ) of the position of the tarsus end at lift-off and touch-down in their respective polar coordinate system (Fig. 2C). Following Wosnitza et al. (2013) and Wahl et al. (2015) we calculated step amplitude rather than stride length. For each leg, we computed the step amplitude (in mm) by averaging the distances between PEP and AEP positions in the ant Cartesian coordinate system. Again, because the path followed by the ant was straight, we averaged the values of the right and left leg of each pair of legs when computing step amplitude.

We studied inter-leg coordination by comparing the time of lift-off of every leg to the time of lift-off of the right mid leg (Wosnitza et al., 2013; Wahl et al., 2015). More precisely, we computed, for each leg, the time lag between the leg lift-off and the last lift-off of the right mid leg. We then divided the value of the time lag by the time elapsed between two successive lift-offs of the right mid leg. This value was expressed as a phase shift between $-\pi$ and π for each leg. Finally, we used circular statistics (Batschelet, 1981) to compute the mean vector of the distribution of the phase shifts for specific groups of ants. As an indication of how ant gait was close to an ideal alternating tripod locomotion, we also computed the tripod coordination strength (TCS) (Wosnitza et al., 2013; Wahl et al., 2015; Ramdya et al., 2017). This index can take values between 0 and 1. A TCS of 1 corresponds to a perfect alternating tripod gait while a TCS of 0 means that the ant performed a completely different type of gait.

Following Moll et al. (2013), we also computed for each ant the change over time of the static stability margin (SSM) during locomotion. For every video frame, the SSM was defined as the minimum distance between the projection of the ant CoM on the horizontal plane and the edges of the polygon formed by all legs in contact with the ground, including the dragged legs. The SSM is positive if the projection of the CoM lies inside the polygon, negative otherwise. We used the expression 'statically stable locomotion' to refer to the parts of the locomotion in which the ant managed to maintain static stability (i.e. when the SSM was positive) and the expression 'statically unstable locomotion' to refer to the parts of the locomotion in which it was not the case (i.e. when the SSM was negative). For each ant, we computed the proportion of time it was performing statically stable locomotion.

In order to investigate whether the decrease in stability we observed in large ants was the same as that one should observe mechanically because of the forward shift of the center of mass of the body or whether this decrease was less than expected because large ants adjusted their gait in order to maintain their stability, we computed a model of an ideal alternating tripod gait and compared the stability data generated by this model to those calculated in real ants. First, we used the allometric relationships we measured between the different body parts of our ants (Table S1, Fig. 3A) to model virtual ants of different sizes. Second, we assumed that all ants walk with the same stepping pattern. We computed the leg position as the mean value of the leg positions observed in our experiment for all ants, corrected for the differences in leg length between ants of different sizes (Table S1, Fig. 3B). Finally, we followed the same procedure as that described above in order to compute the proportion of statically stable locomotion for these virtual ants. The data we obtained with these virtual ants were then compared with those obtained in real ants.

For the unloaded condition, all variables y were expressed as a power law function of ant mass M: $y=a\times M^b$. For each variable, we give the value of the coefficients a and b, as well as the value of the variables predicted by the statistical model for the mean ant mass (11.8 mg). For the loaded condition, because we tested the same ants first loaded and then unloaded, we computed for each variable the ratio of its value between the loaded (y_l) and unloaded (y_u) condition and expressed it as a power law function of both ant mass (M) and LR: $y_l/y_u=c\times M^d\times LR^e$. For each variable, we give the value of the coefficients c, d and e as well as the value of the ratio predicted by the statistical model for mean ant mass and a load ratio of one. A positive value for a coefficient (i.e. c, d or e) means that the value of the response variable in loaded condition increases compared with unloaded condition when the explanatory variable increases and vice versa.
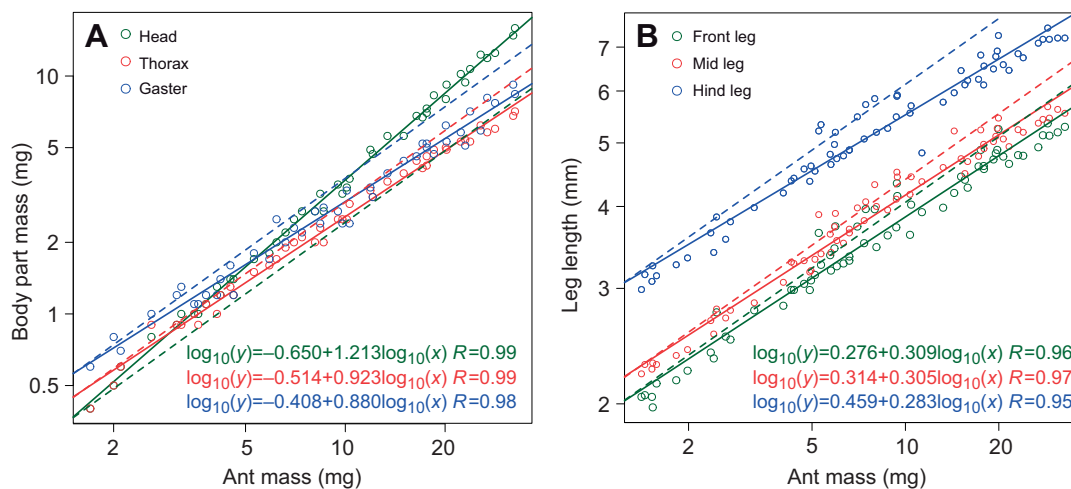

Fig. 3. Mass of body parts and leg length as a function of ant mass. (A) Relationship between the mass of the three main body parts of the ants and their mass. The solid lines represent the regression model for head (green), thorax (red) and gaster (blue). The dashed lines correspond to a slope of 1 with unchanged elevation for each body part, i.e., what would be expected in absence of allometry. N=45 ants. (B) Relationship between the length of the ant legs and their mass. The solid lines represent the regression model for front (green), mid (red) and hind (blue) legs (see Table S1). The dashed lines correspond to a slope of 1/3 with unchanged elevation for each leg, i.e. what would be expected if large ants had proportionally longer legs than small ants. Data from Felden (2014). N=65 ants.

In panel A: $\log_{10}(y)=-0.650+1.213\log_{10}(x)$ R=0.99; $\log_{10}(y)=-0.514+0.923\log_{10}(x)$ R=0.99; $\log_{10}(y)=-0.408+0.880\log_{10}(x)$ R=0.98.

In panel B: $\log_{10}(y)=0.276+0.309\log_{10}(x)$ R=0.96; $\log_{10}(y)=0.314+0.305\log_{10}(x)$ R=0.97; $\log_{10}(y)=0.459+0.283\log_{10}(x)$ R=0.95.

We performed all data analysis and designed all graphics with R (v. 3.5.1) run under RStudio (v. 1.0.136). The dataset used for this study is available at http://doi.org/10.5281/zenodo.2646485

RESULTS

Unloaded ants: influence of body mass

Stride frequency ($F_{1,43}$=59.92, P<0.001) decreased with ant mass (Table 1). However, step amplitude increased with ant mass for every leg (front leg: $F_{1,43}$=204.45, P<0.001; mid leg: $F_{1,43}$=193.57, P<0.001; hind leg: $F_{1,43}$=122.73, P<0.001). As a result, speed did not depend on ant mass ($F_{1,43}$=0.33, P=0.566). The duty factor of all legs increased with increasing ant mass, particularly for the front ($F_{1,43}$=37.04, P<0.001) and mid ($F_{1,43}$=23.06, P<0.001) legs (Fig. S1A–C). Therefore, compared with small ants, large ants tended to have more legs in contact with the ground during a stride ($F_{1,43}$=37.28, P<0.001). The front and mid legs were almost never dragged by ants. However, independent of ant mass, hind legs were dragged during 21% of a stride on average.

In an ideal alternating tripod gait, all legs of a tripod lift-off simultaneously. In actual locomotion however, there is no such perfect synchronization. Nevertheless, the alternating tripod gait model still holds if the time interval between the lift-off of the three legs of the same tripod is small. Fig. 4A shows that the ants' gait is very close to an ideal tripod gait (see also Fig. S2A). However, for large ants, the front legs tended to lift-off slightly after the mid and hind legs of the same tripod. As a result, the TCS slightly decreased ($F_{1,43}$=13.43, P<0.001).

Fig. 5A shows the Cartesian coordinates of the legs expressed in units of body length for three categories of ants based on their mass both at lift-off (PEP, on the left) and at touch-down (AEP, on the right). All legs were positioned at a greater distance from their point of insertion in the body with increasing ant mass both at touch-down (AEP: front legs: $F_{1,43}$=1572.03, P<0.001; mid legs: $F_{1,43}$=1212.90, P<0.001; hind legs: $F_{1,43}$=670.01, P<0.001) and lift-off (PEP: front legs: $F_{1,43}$=207.43, P<0.001; mid legs: $F_{1,43}$=870.76, P<0.001; hind legs: $F_{1,43}$=1060.18, P<0.001). The angle between the front leg and the longitudinal axis (Fig. 2) at touch-down tended to decrease with ant mass (AEP: $F_{1,43}$=15.47, P<0.001) while, at lift-off, the angle between the leg and the longitudinal axis slightly increased with ant mass for all three legs (PEP: front legs: $F_{1,43}$=11.48, P=0.002; mid legs: $F_{1,43}$=7.77, P=0.008; hind legs: $F_{1,43}$=19.86, P<0.001).

The static stability margin decreased during a stride and reached a local minimum value just before touch-down of one of the front legs (Fig. 6A,B). The percentage of time an ant moved in statically stable locomotion (i.e. with an SSM<0) decreased with ant mass ($F_{1,43}$=4.96, P=0.031). This can be explained by the forward shift in the horizontal position of the CoM in ants of increasing size ($F_{1,43}$=85.77, P<0.001). When the SSM was negative, it was always due to the CoM being in an anterior position to the polygon of support. Therefore, small ants have generally a more balanced locomotion than large ants.

Table 1. Influence of body mass on the kinematics of unloaded ants

	Variable	Model prediction for mean ant mass [CI]	Coefficient a [CI]	Coefficient b for ant mass [CI]	Adj. R^2
Global kinematics	Speed (mm s^{-1})	29.22 [27.16; 31.43]	27.73 [24.20; 31.77]	0.017 [−0.042; 0.075]	0.01
	Stride frequency	3.988 [3.756; 4.234]	7.097 [6.346; 7.936]	−0.184 [−0.232; −0.136] *	0.57
	Stride amplitude				
	Front leg (mm)	4.289 [4.103; 4.485]	1.819 [1.674; 1.977]	0.274 [0.238; 0.309] *	0.84
	Mid leg (mm)	4.990 [4.773; 5.216]	2.318 [2.134; 2.518]	0.245 [0.209; 0.280] *	0.81
	Hind leg (mm)	3.688 [3.520; 3.864]	1.938 [1.776; 2.115]	0.205 [0.168; 0.243] *	0.73
Gait	Duty factor				
	Front legs	0.653 [0.641; 0.665]	0.569 [0.550; 0.589]	0.044 [0.029; 0.058] *	0.45
	Mid legs	0.691 [0.677; 0.705]	0.612 [0.589; 0.636]	0.039 [0.022; 0.055] *	0.33
	Hind legs	0.625 [0.603; 0.648]	0.569 [0.533; 0.609]	0.030 [0.001; 0.058] *	0.07
	Proportion of time hind legs dragged	0.209 [0.178; 0.246]	0.251 [0.186; 0.340]	−0.059 [−0.189; 0.071]	0.02
	Mean no. of legs in contact with ground	4.392 [4.335; 4.450]	3.980 [3.885; 4.078]	0.031 [0.021; 0.042] *	0.45
	Tripod coordination strength (TCS)	0.591 [0.550; 0.636]	0.823 [0.718; 0.942]	−0.105 [−0.163; −0.047] *	0.22
Leg positioning	AEP				
	Front legs r (mm)	5.122 [5.020; 5.225]	1.912 [1.842; 1.985]	0.314 [0.298; 0.330] *	0.97
	Front legs φ (deg)	154.4 [152.7; 156.2]	163.3 [159.9; 166.8]	−0.018 [−0.027; −0.009] *	0.25
	Mid legs r (mm)	5.704 [5.578; 5.833]	2.165 [2.077; 2.258]	0.309 [0.291; 0.327] *	0.96
	Mid legs φ (deg)	108.1 [106.4; 109.9]	111.6 [108.2; 115.1]	−0.010 [−0.023; 0.003]	0.03
	Hind legs r (mm)	4.970 [4.815; 5.131]	1.784 [1.681; 1.894]	0.327 [0.301; 0.352] *	0.94
	Hind legs φ (deg)	46.47 [45.01; 47.97]	47.83 [45.06; 50.76]	−0.009 [−0.035; 0.016]	0.01
	PEP				
	Front legs r (mm)	2.208 [2.049; 2.380]	0.578 [0.502; 0.664]	0.428 [0.368; 0.487] *	0.82
	Front legs φ (deg)	98.42 [93.92; 103.1]	80.84 [74.09; 88.20]	0.063 [0.025; 0.100] *	0.19
	Mid legs r (mm)	6.271 [6.115; 6.430]	2.492 [2.378; 2.612]	0.294 [0.274; 0.314] *	0.95
	Mid legs φ (deg)	58.07 [56.39; 59.81]	52.45 [49.65; 55.41]	0.033 [0.009; 0.056] *	0.13
	Hind legs r (mm)	8.028 [7.864; 8.196]	3.473 [3.342; 3.610]	0.267 [0.251; 0.284] *	0.96
	Hind legs φ (deg)	29.29 [28.26; 30.30]	24.03 [22.48; 25.69]	0.063 [0.035; 0.092] *	0.30
Static stability	Mean x position of CoM (BL)	0.283 [0.271; 0.295]	0.172 [0.159; 0.187]	0.158 [0.123; 0.192] *	0.66
	Proportion of statically stable locomotion	0.947 [0.933; 0.962]	0.988 [0.960; 1.017]	−0.014 [−0.026; −0.001] *	0.08

Each line gives the results of a power law model describing the influence of ant mass M (in mg) on each kinematics variables studied y, following the equation $y=a×M^b$. The first column corresponds to the model prediction and 95% CI for the mean value of ant mass (11.8 mg). The second column gives the value of the coefficient a and its 95% CI, the third column the value of the coefficient b for ant mass and its 95% CI and the fourth column the adjusted R^2 for the model. BL, body length. * indicates that 0 is not included in the 95% CI of the coefficient b for ant mass. Because the path followed by ants was straight, the values of the variables for the right and left leg of each pair of legs were averaged. N=45 ants.
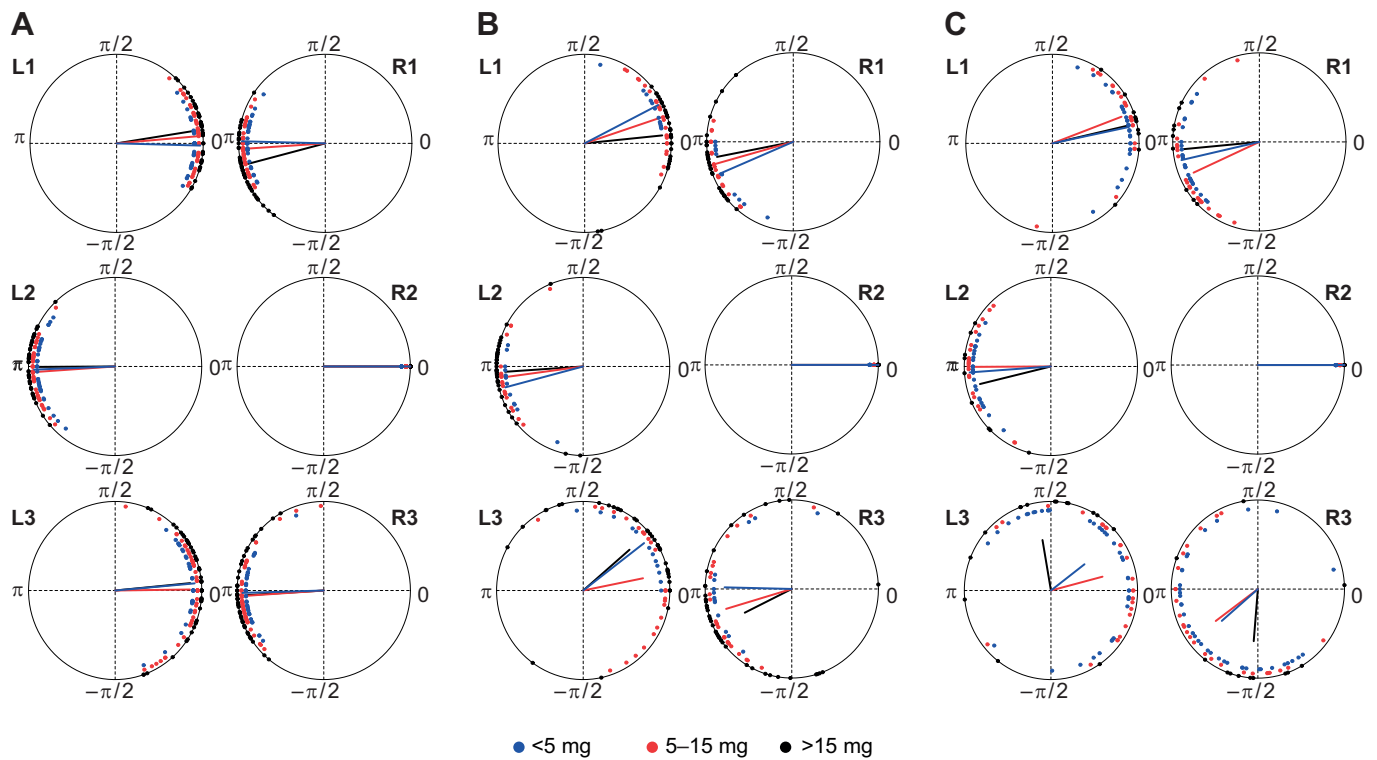
Fig. 4. Phase plots of lift-off onset of all legs with respect to the right mid leg (R2). (A) Unladen ants ($N_{<5mg}$=13; N_{5-15mg}=16; $N_{>15mg}$=15). (B) Loaded ants with load ratio (LR)≤3.5 ($N_{<5mg}$=4; N_{5-15mg}=9; $N_{>15mg}$=12). (C) Loaded ants with LR>3.5 ($N_{<5mg}$=9; N_{5-15mg}=7; $N_{>15mg}$=3). R, right; L, left; blue, data for small ants (<5 mg); red, data for intermediate ants (5–15 mg); black, data for large ants (>15 mg); lines show mean vector of angle distribution; length is equal to mean vector length and is inversely proportional to dispersion (Batschelet, 1981).

Whether large ants are able to adjust their locomotory behavior to compensate, at least partly, for the decrease in stability as a result of their CoM being placed in a more forward position can be assessed by our ideal alternating tripod gait model. The coefficient *a* describing the influence of ant mass on the proportion of time our model ants perform statically stable locomotion is −0.092 [CI: −0.132; −0.051]. This value is significantly smaller than that found in real ants (−0.014 [CI: −0.026; −0.001], see Table 1). Thus, if all ants were walking with the same ideal alternating tripod gait, the effect of the forward shift of the CoM on the proportion of time large ants perform statically stable locomotion would be more important than what we observed in our experiment. We conclude that the changes observed above in the kinematics features of locomotion between small ants and large ants lead to an increase in static stability in large ants.

Loaded ants: influence of ant body mass and load ratio

Fig. 7 and Table 2 show the values of load ratio (LR) tested for ants of different body masses. Depending on the value of the LR, ants exhibited two kinds of behaviors when loaded. They could either keep the load lifted above the ground during locomotion or they could maintain their head in a very slanted position and push the load in front of them (see Movies 1–3 for illustrations). We called the first behavior 'carrying' and the second 'pushing'. The criteria we used to distinguish between the two behaviors is based on whether or not the load glued on the ant mandibles was in contact with the ground during locomotion. We used a logistic regression to investigate the effect of ant mass, LR and the interaction between these two variables, on the probability of using pushing versus carrying behavior to transport the load. The results show a

marginally significant interaction between ant mass and LR (z=−1.985, P=0.047). Pushing generally occurred for LR>5 for ants weighing >10 mg, while for ants of lower body mass, both carrying and pushing could be observed for LR>4. We will only consider ants that carry their load in the following analyses.

Independent of ant mass, stride frequency decreased with increasing LR ($F_{2,42}$=21.58, P<0.001; Fig. S3A). Step amplitude was independent of LR for front and mid legs but tended to decrease for hind legs ($F_{2,42}$=2.96, P=0.062). Consequently, ant speed decreased with increasing LR ($F_{2,42}$=21.58, P<0.001; Fig. S3B). However, for ants transporting equivalent loads there was no effect of body mass on both stride frequency and step amplitude.

Independent of ant mass, the duty factor increased for the front ($F_{2,42}$=58.32, P<0.001), mid ($F_{2,42}$=25.41, P<0.001) and hind legs ($F_{2,42}$=11.71, P<0.001) for increasing load ratios (Fig. S1D–F). The mean number of legs simultaneously in contact with the ground increased for increasing load ratios independent of ant size and, to a lesser extent, increased for increasing body mass independent of load ratio ($F_{2,42}$=56.94, P<0.001). Similarly to when ants were unloaded, the front and mid legs were almost never dragged during locomotion when ants were loaded. The proportion of time the hind legs were dragged decreased significantly as soon as the ant was loaded, with no influence of either ant mass or load ratio.

Fig. 5B shows the changes in leg positions in unit of body length at lift-off (PEP, on the left) and touch-down (AEP, on the right) for ants carrying either small (LR<3.5) or large (LR>3.5) relative loads. Independent of ant mass, the angle between the front legs and the longitudinal axis increased with increasing load ratio at lift-off (PEP: $F_{2,42}$=3.53, P=0.038). Ants also placed their mid legs further away from the body at touch-down (AEP: $F_{2,42}$=6.03, P=0.005) and
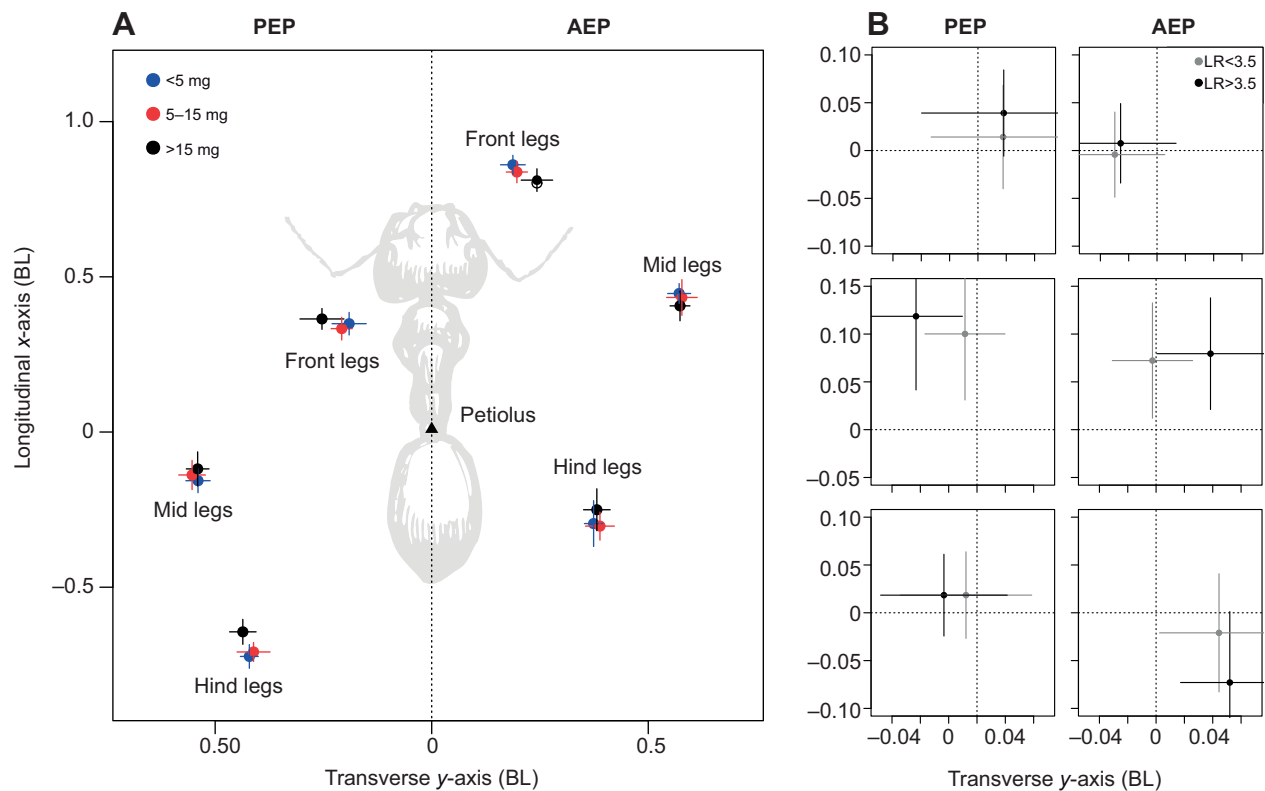
Fig. 5. Footfall geometry of ants during locomotion. (A) Unloaded ants; the mean position of the front, mid and hind legs during lift-off (posterior extreme position, PEP) and touch-down (anterior extreme position, AEP) along with their s.d. is shown for different ranges of ant body masses ($N_{<5mg}$=13, N_{5-15mg}=16, $N_{>15mg}$=16). (B) Loaded ants; changes in leg positions at PEP and AEP when ants were walking loaded compared with when they were walking unloaded. The origin corresponds to the leg position for unloaded ants. The average change in position over three strides along with their s.d. is shown. Ants were categorized in two groups depending on load ratio ($N_{LR<3.5}$=26, $N_{LR>3.5}$=19). The scale is in units of body length (BL).

the angle between the mid legs and the longitudinal axis slightly increased with LR at lift-off (PEP: $F_{2,42}$=3.45, P=0.041). Independent of ant mass, the hind legs were placed further away from the body with increasing LR at touch-down (AEP: $F_{2,42}$=3.45, P=0.041) and the angle with the body longitudinal axis increased with increasing ant mass independent of LR (AEP: $F_{2,42}$=4.73, P=0.014). Finally, at lift-off the angle of the hind legs increased with LR independent of ant mass and increased with ant mass independent of LR (PEP: $F_{2,42}$=5.65, P=0.007).

While performing loaded locomotion, ants did not exhibit the same inter-leg coordination pattern than during unloaded locomotion (Fig. 4). First, there was more dispersion in phase shift between legs for loaded ants, especially for the hind legs and for high LR values (>3.5, see Fig. 4B2). Second, the three legs of the same tripod tended to lift-off in a specific order (i.e. mid leg→front leg→hind leg). This was especially clear for the hind leg, which was the last to lift-off in each tripod. This order seems to be more strictly followed for higher LR values and for large ants (Fig. 4B2). As a result, the value of TCS decreased for increasing LR ($F_{2,42}$=12.48, P<0.001).

Independent of ant size, the percentage of time ants were performing statically stable locomotion decreased with increasing LR in loaded ants ($F_{2,42}$=34.05, P<0.001). When the minimum static stability margin became negative, it was always because the CoM was anterior to the polygon of support.

DISCUSSION

In this study, we investigated the kinematics of locomotion of unloaded and loaded ants of the polymorphic species *M. barbarus*.

We found that, relative to their size, small ants were able to carry larger loads than large ants. Small ants also were more stable than large ants; all ants, whatever their size, reduced their speed when carrying loads of increasing mass. The locomotion of unloaded ants was very close to an ideal alternating tripod gait. This allowed them to perform a rather statically stable locomotion. On the other hand, loaded ants were mostly statically unstable and their gait changed to more tetrapod-like locomotion, wave gait locomotion and hexapodal stance phases (see Fig. S2B for an illustration).

Unloaded ants

In *M. barbarus*, large ants have, relative to their size, larger heads than small ants (Heredia and Detrain, 2000; Bernadou et al., 2016). This means that their center of mass is located in a more anterior position compared with small ants. Large ants are thus more likely to be off balance than small ants. Nevertheless, our ideal alternating tripod gait model shows that, somehow, they are able to compensate for the instability caused by the forward shift of their center of mass. Our results suggest that this could be done through a change in leg positioning and gait parameters. For example, large ants lifted off their front legs at a position further away from their body than small ants. Note however, that the increase of the front leg distance from the body with ant mass (i.e. 0.428 [0.368; 0.487], see Table 1) is significantly greater than what would be expected by the allometric relationship between front leg length and ant mass (i.e. 0.310 [0.295; 0.325], see Table S1). In other words, large ants lifted off their front legs relatively further away from the coxae than small ants. In addition, at lift-off, the angle between the front legs and the longitudinal axis increased with ant mass. Therefore, the front legs
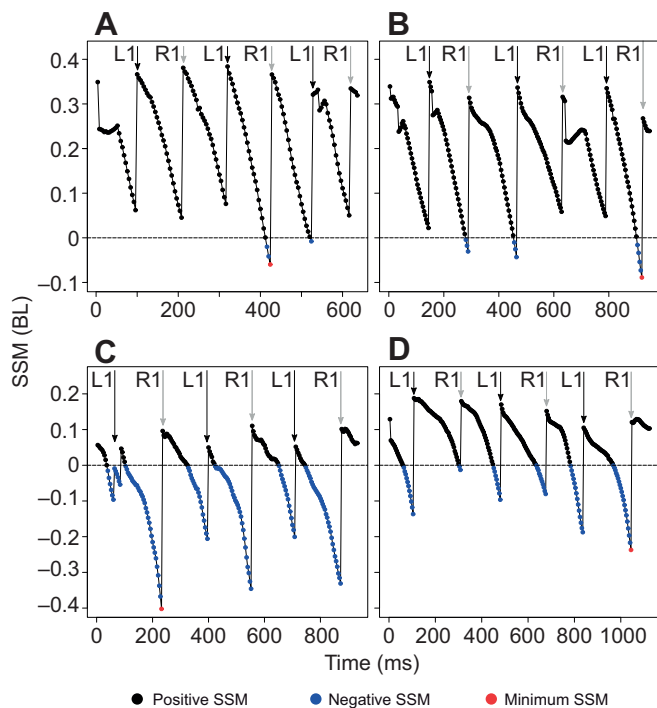
Fig. 6. Time variation of the static stability margin (SSM). The value of SSM for unloaded (A,B) and loaded (C,D) ants, normalized by body length, is shown during three consecutive strides for a small ant (A,C) (ant mass=4.2 mg, LR=5.0) and a large ant (B,D) (ant mass=32.1 mg, LR=2.0). Black and gray arrows represent R1 and L1 touched down, respectively.

lifted off in a more anterior position in large ants than in small ants. The position of the front legs at lift-off is of crucial importance for static stability since the minimum values of SSM arise just before the contralateral front leg touches down (Fig. 6). Consequently, lifting off the front leg in a more anterior position allows large ants to decrease the proportion of unstable static locomotion. This leads to a decrease in relative step amplitude for front legs with increasing ant mass (again by comparing the respective coefficients in Table 1 for the step amplitude of front legs and in Table S1 for the relationship between front leg length and ant mass). In addition, the
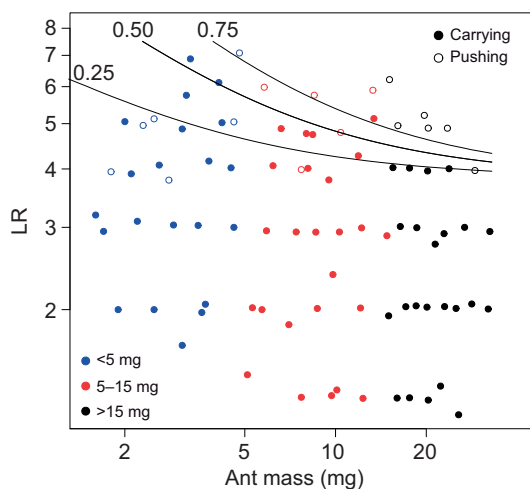
Fig. 7. Transportation method used by ants during locomotion. Probability of pushing a load as a function of ant mass and load ratio. The lines of equal probability were calculated by a logistic regression model (N=86 ants).

duty factor increased for all legs, which means that large ants kept their legs in contact with the ground for a proportionally longer time during a stride than small ants. As a result, the mean number of legs in contact with the ground increased with increasing ant mass, which contributes to increase static stability in large ants. In conclusion, the differences in morphology between ants of different sizes do induce a less statically stable locomotion in large ants but this effect is reduced by the fact that they are able to adjust their stepping pattern to compensate, at least partly, for this instability.

Carrying capacity

Carrying capacity, defined here as the value of the load ratio for which the transition (i.e. the 50% probability) between carrying and pushing occurred, was greater for small ants than for large ants (Fig. 7). Therefore, small ants were able to carry relatively heavier loads than large ants. This is concordant with the results obtained by Bernadou et al. (2016) in the same species. However, in their study, the carrying capacity was related to the transition occurring between carrying and dragging, not between carrying and pushing as in our study. To our knowledge, pushing behavior has never been described in field observations of foraging seed-harvesting ants. Pushing probably occurs very rarely in the field because of the friction forces generated by the heterogeneities of the natural substrate on which the ants are moving. These friction forces would rapidly lead ants to abandon altogether their load or turn around and start dragging it while moving backward to their nest. Pushing is probably an artefact caused by both the gluing of the load on the ants' mandibles and the smoothness of the substrate on which the ants are moving.

The differences in load-carrying capacity can be accounted for by two non-exclusive explanations. The first is related to the well-known scale effect, while the second is related to differences in the locomotion and/or the morphology (induced by allometric relationships) of ants of different sizes.

The scale effect is due to the fact that the muscle force of an animal depends on its muscle cross-sectional area, which increases with the square of linear body dimensions while body mass increases with the cube (Schmidt-Nielsen, 1984; Dial et al., 2008). This would lead to a reduction in relative load capacity in large ants compared with small ants. However, this reasoning would hold only if large ants were a simple enlargement of small ones, i.e. if their body parts grew isometrically. As mentioned before, this is not exactly the case in *M. barbarus*: compared with small ants, large ants not only have relatively larger heads (Table S1, Bernadou et al., 2016, Fig. 3A) but they have also relatively shorter legs (Table S1, Fig. 3B, Felden, 2014). Nonetheless, the scale effect could still apply to some extent. To assess its importance, we compared our data on load-carrying capacity in ants of different sizes with those that would be expected if the predictions of the scale effect were computed on ants of different sizes but with same morphology. Since the scale effect always refers to a comparison between two individuals of different mass, we chose as a reference an ant weighing 1.5 mg (corresponding to the smallest ant observed in our colony with a carrying capacity of 8.9, see Fig. 7). Then, an ant of a given mass M would be ($M/1.5$) heavier than the reference ant and, according to the scale effect, its muscle section (and thus muscular power) would be $(M/1.5)^{2/3}$ larger. An ant of mass M would thus be able to carry a load up to:

$$\left(\frac{M}{1.5}\right)^{2/3} \times (8.9 - 1) \times 1.5 \text{ mg},$$

Table 2. Influence of body mass and load ratio on the changes in kinematics between unloaded and loaded locomotion

	Variable loaded/unloaded	Model prediction for mean ant mass and LR=1 [CI]	Coefficient a [CI]	Coefficient b for ant mass [CI]	Coefficient c for load ratio [CI]	Adj R^2
Global kinematics	Speed (mm s⁻¹)	1.036 [0.826; 1.300]	1.224 [0.814; 1.841]	−0.0669 [−0.1756; 0.0418]	−0.646 [−0.856; −0.437]*	0.48
	Stride frequency	0.979 [0.842; 1.140]	1.045 [0.796; 1.373]	−0.0261 [−0.0987; 0.0465]	−0.396 [−0.535; −0.256]*	0.45
	Stride amplitude					
	Front leg (mm)	1.015 [0.900; 1.145]	1.138 [0.916; 1.414]	−0.0460 [−0.1038; 0.0118]	−0.051 [−0.162; 0.061]	0.01
	Mid leg (mm)	0.996 [0.875; 1.135]	0.987 [0.781; 1.248]	0.0038 [−0.0587; 0.0662]	−0.047 [−0.167; 0.074]	0.02
	Hind leg (mm)	1.060 [0.918; 1.223]	1.055 [0.815; 1.367]	0.0016 [−0.0671; 0.0704]	−0.138 [−0.270; −0.005]*	0.08
Gait	Duty factor					
	Front legs	0.989 [0.949; 1.032]	0.964 [0.894; 1.040]	0.0104 [−0.0097; 0.0305]	0.190 [0.151; 0.228]*	0.72
	Mid legs	1.002 [0.951; 1.055]	0.942 [0.858; 1.035]	0.0245 [0.0001; 0.0493]	0.164 [0.117; 0.212]*	0.53
	Hind legs	1.043 [0.957; 1.137]	0.963 [0.825; 1.124]	0.0321 [−0.0090; 0.0733]	0.187 [0.108; 0.266]*	0.33
	Proportion of time hind legs dragged	0.349 [0.178; 0.684]	0.268 [0.080; 0.898]	0.1067 [−0.2152; 0.4286]	−0.191 [−0.810; 0.429]	0.02
	Mean no. legs in contact with ground	0.951 [0.920; 0.984]	0.893 [0.841; 0.948]	0.0257 [0.0097; 0.0417]*	0.159 [0.129; 0.190]*	0.72
	Tripod coordination strength (TCS)	1.226 [0.867; 1.732]	1.920 [1.011; 3.649]	−0.1806 [−0.3548; −0.0063]*	−0.803 [−1.130; −0.476]*	0.36
Leg positioning	AEP					
	Front legs r (mm)	0.960 [0.907; 1.017]	0.980 [0.884; 1.086]	−0.0082 [−0.0356; 0.0192]	0.018 [−0.035; 0.071]	0.01
	Front legs φ (deg)	1.005 [0.978; 1.033]	0.979 [0.932; 1.028]	0.0107 [−0.0023; 0.0237]	0.014 [−0.011; 0.039]	0.02
	Mid legs r (mm)	0.986 [0.937; 1.038]	0.966 [0.881; 1.058]	0.0085 [−0.0159; 0.0330]	0.077 [0.030; 0.124]*	0.19
	Mid legs φ (deg)	1.055 [1.012; 1.100]	1.048 [0.972; 1.130]	0.0027 [−0.0174; 0.0228]	−0.001 [−0.040; 0.038]	0.01
	Hind legs r (mm)	1.004 [0.935; 1.078]	0.988 [0.869; 1.122]	0.0065 [−0.0275; 0.0404]	0.106 [0.041; 0.172]*	0.20
	Hind legs φ (deg)	1.049 [0.940; 1.170]	0.898 [0.738; 1.094]	0.0622 [0.0099; 0.1146]*	−0.025 [−0.126; 0.076]	0.14
	PEP					
	Front legs r (mm)	0.904 [0.767; 1.065]	0.974 [0.725; 1.308]	−0.0300 [−0.1085; 0.0486]	−0.016 [−0.167; 0.135]	0.02
	Front legs φ (deg)	0.923 [0.815; 1.046]	0.844 [0.674; 1.055]	0.0364 [−0.0231; 0.0960]	0.151 [0.036; 0.266]*	0.10
	Mid legs r (mm)	0.911 [0.853; 0.973]	0.881 [0.782; 0.992]	0.0134 [−0.0182; 0.0450]	0.040 [−0.021; 0.101]	0.02
	Mid legs φ (deg)	1.062 [0.982; 1.149]	1.039 [0.902; 1.197]	0.0091 [−0.0286; 0.0467]	0.089 [0.017; 0.162]*	0.10
	Hind legs r (mm)	1.001 [0.965; 1.039]	0.998 [0.934; 1.066]	0.0012 [−0.0164; 0.0188]	0.005 [−0.029; 0.039]	0.01
	Hind legs φ (deg)	0.938 [0.854; 1.030]	0.794 [0.670; 0.940]	0.0670 [0.0219; 0.1120]*	0.120 [0.033; 0.206]*	0.17
Static stability	Mean x position of CoM (BL)	1.497 [1.377; 1.629]	2.190 [1.883; 2.548]	−0.1530 [−0.1932; −0.1127]*	0.367 [0.290; 0.445]*	0.87
	Proportion of statically stable locomotion	1.299 [1.030; 1.639]	1.503 [0.989; 2.284]	−0.0585 [−0.1699; 0.0528]	−0.814 [−1.028; −0.599]*	0.60

Each line gives the result of a power law model describing the influence of ant mass M (in mg) and load ratio (LR) on the relative changes of kinematics variables y between the loaded and unloaded condition. The corresponding equation is $y/y_u=c×M^d×LR^e$, where y_u corresponds to the value of the kinematic variable in the unloaded condition and y_l to the value of the same variable in the loaded condition. The first column corresponds to the model prediction and 95% confidence interval for the mean value of ant mass (11.8 mg) and a load ratio of 1 (unloaded ants). The second column gives the value of the coefficient c and its 95% CI, the third column the value of the coefficient d for ant mass and its 95% CI, the fourth column the value of the coefficient e for the load ratio and its 95% CI and the fifth column the adjusted R^2 for the model. A positive value for a coefficient means that the value of the response variable in loaded condition increases compared with unloaded condition when the explanatory variable increases and vice versa. BL, body length. * indicates that 0 is not included in the 95% CI of the coefficient d for ant mass and e for load ratio. Because the path followed by ants was straight, the values of the variables for the right and left leg of each pair of legs were averaged. N=45 ants.

which, after applying the formula for the calculation of load ratio, leads to a carrying capacity of:

$$1 + 1.5^{1/3} \times (8.9 - 1)M^{-1/3} = 1 + 9M^{-1/3},$$

which is the equation of the black line in Fig. 8. As can be seen in Fig. 8, the predictions of the carrying capacity for our model ants of different sizes with same morphology is close to the curve representing the 50% probability of carrying a load versus pushing it that we obtained from our experiment. It is also close to the curve representing the 50% probability of carrying a load versus dragging it from the field experiments by Bernadou et al. (2016) in which the ants transported food items of various sizes deposited on their foraging trails. Therefore, it seems that ants start pushing in our experiment for about the same load ratio values as they start dragging in Bernadou et al. (2016) and that this can be explained mainly by the scale effect.

Nonetheless, one cannot exclude that the differences observed in the locomotor behavior between small and large ants could also partly explain the differences in carrying capacity. Table 2 indeed points out some differences in the kinematics of ants of different sizes, independent of load ratio. However, despite slight changes in the mean number of legs in contact with the ground, TCS values and hind leg positioning with increasing ant mass, we could not find any particular logic that could help to explain the differences in carrying capacity between small and large ants. Therefore, it seems to us that the observed differences in carrying capacities in ants of different sizes can be well explained by the scale effect. Note that a recent study in *Atta cephalotes* found exactly the opposite result: that the carrying capacity is constant and independent of ant mass (Segre and Taylor, 2019). Further studies are needed in order to determine the origin of these differences.

Influence of load ratio on locomotion

The main effect of carrying a load for an ant is to shift its CoM forward. As a consequence, the CoM is located closer to the front edge of the polygon of support, or even lies out of it, and the SSM decreases or becomes negative, leading the ant to perform less

Fig. 8. Ant carrying capacities and scale effect prediction. The purple line represents 50% probability of carrying the load versus pushing it (our data); the green line represents 50% probability of carrying the load versus dragging it (data from Bernadou et al., 2016); in both cases, the dashed lines represent 25% and 75% probabilities; the black line represents the prediction of load carrying capacity based on scale effect and a 1.5 mg ant reference.

statically stable or statically unstable locomotion. Moll et al. (2013) showed that loaded *A. vollenweideri* ants can reduce this effect by changing the way they carry their load: by carrying the pieces of grass blade they hold in their mandibles in a more upward, backward-tilted position they can shift their CoM in a somewhat backward position. This is of course impossible in our experiment because ants cannot adjust the position of the load glued on their mandibles. This would not happen either in the field because most seeds collected by *M. barbarus* are not elongated enough to be carried in the same way as pieces of grass blades in grass-cutting ants. The CoM of loaded *M. barbarus* workers is thus shifted forward and the percentage of time their locomotion is statically unstable during a stride increases for increasing LR (Table 2), reaching up to 90% for the highest LRs.

Such statically unstable locomotion has already been reported for insects in the literature. For instance, the cockroach *Blaberus discoidalis*, when moving at very high speed, often performs statically unstable locomotion and thus maintains its balance through dynamic stability (Ting et al., 1994; Koditschek et al., 2004). Dynamic stability refers to individuals keeping their balance when statically unstable by only briefly 'falling' forward before new supporting legs contact the ground (Moll et al., 2013). Statically unstable locomotion has also been observed by Moll et al. (2013) in loaded workers of the grass cutting ant *A. vollenweideri*. These authors have suggested that loaded ants could use dynamic stability in order to avoid falling over during the statically unstable part of their locomotion (Moll et al., 2010, 2013).

However, loaded *M. barbarus* workers move too slowly (Table 2) to maintain their balance through dynamic stability: they would fall forward before the front leg catches up. Rather, we assume that they maintain their balance by clinging to the ground with the tarsal claws located at the end of their mid and hind legs. Indeed, scanning electron microscope images of the substrate texture show that the claws can easily cling to the paper fibers (Fig. S4B). Consequently, they tend to keep more legs in contact with the ground for increasing LRs. This leads to a decrease in their stride frequency and TCS and to an increase of the duty factor of all legs (Table 2). Hind legs are of particular importance in keeping the ant balanced because they have a higher lever-arm effect. In our experiment, the percentage of time the hind legs were dragged decreased as soon as the ant was loaded independent of ant mass and load ratio (mean±CI$_{0.95}$: −12.1±8.2%), probably because ants use the claws of the pretarsus in order to cling to the ground. In this respect, it would be interesting to investigate how ants maintain their balance when their adhesive prestarsal structures are blocked or when they walk on a slipping substrate (see Ramdya et al., 2017 for an example in *Drosophila melanogaster*). The tendency for the hind legs to lift-off after the front legs touched down also increased for increasing load ratio (Fig. 4B,C). This is coherent with the balance strategy used by ants, as the SSM is maximal at front leg touch-down (Fig. 6C,D) and thus it is less risky to lift-off the hind leg at this time. Finally, as a result of the stride frequency decrease (and because step amplitude remains constant), the speed decreased with increasing LR, which is concordant with most studies in other load-carrying ants, such as *Atta colombica* (Lighton et al., 1987), *A. vollenweideri* (Röschard and Roces, 2002), *Atta cephalotes* (Burd, 2000) and *Veromessor pergandei* (Rissing, 1982).

Reinhardt and Blickhan (2014a) showed that, during steady state locomotion, *Formica polyctena* uses mainly its hind legs in order to generate propulsion forces while Wöhrl et al. (2017) showed in *Cataglyphis fortis* that it is the mid legs that are mainly used for propulsion. In both cases however, the front legs have a brake effect
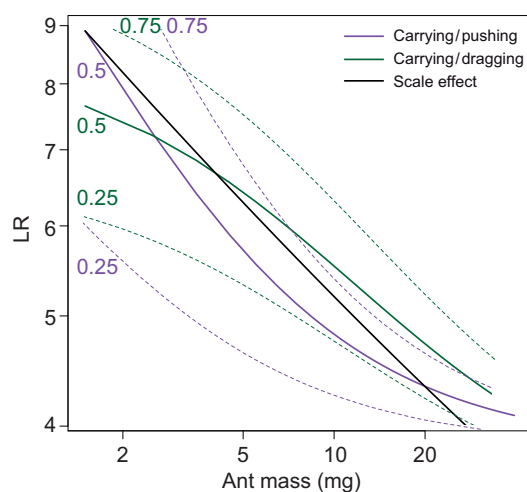
on locomotion. To our knowledge, there are no studies so far that measured the ground reaction forces (GRFs) in loaded ants. Nonetheless, it is possible to infer the propulsion behavior of the legs in our experiment based on the position of their tarsi. Indeed, as shown by Endlein and Federle (2015), depending on the GRFs, the tarsi attach differently to the substrate. The morphology of the tarsal attachment of *M. barbarus* (Fig. S4A) is comparable to that of other ants (Federle et al., 2001; Endlein and Federle, 2008). It seems thus fair to assume that they cling to the substrate in a similar way. Like Endlein and Federle (2015), we observed in our videos two positions for the hind leg tarsi during the stance phase: on 'heels', during the first part of the stance phase, and on 'toes', during its second part (Fig. S5). This would suggest that hind legs have a 'compression and pushing' action in the first part of the stance phase, i.e. participate to propulsion, and then have a 'tension and pulling' action on the last part of the stance phase, acting as a holding point for the ants not to fall over. For mid legs, the tarsi were usually in the 'heel' position and were thus likely to participate in propulsion. These observations are purely qualitative as the resolution of our videos makes a quantitative analysis of these data tricky. The use of a miniature force plate (Bartsch et al., 2007; Reinhardt and Blickhan, 2014b) to compare the GRFs of unloaded and loaded ants would provide crucial insights on how the different legs of the ants contribute to the stability and propulsion of loaded locomotion.

Conclusion

We have shown in this study that unloaded *M. barbarus* workers display different gaits depending on their body mass. For large ants, these differences seem to be mainly explained by a compensation for the imbalance caused by their disproportionally larger head. Small ants are able to carry proportionally heavier loads than large ants and scale effect provides a simple and satisfactory explanation for this difference. Moreover, our results show that loaded ants are often statically unstable during locomotion and that they maintain their balance by clinging to the ground. Further studies are required to determine the contribution of each leg to both stability and propulsion.

Large ants are more costly to produce than small ants. So why do colonies produce them if they are less efficient in transporting loads? One answer to this question is that, although large ants have lower load carriage performance than small ants, they are nonetheless able to carry on average loads of higher masses than small ants and to seize and transport items of larger diameters with their large and powerful mandibles (fig. 3 in Bernadou et al., 2016). This could allow colonies to increase the size range of the food items retrieved to the nest so that they can enlarge their diet breadth and better match the size distribution of the food resources available in their environment (Davidson, 1978). Large ants may also play roles other than foraging in seed-harvesting ant colonies, such as removing the obstacles encountered on foraging trails, constructing and defending the nest (Rissing, 1982), cutting thick plant stalks or milling the seeds inside the nest to prepare them for consumption. The significance of our results for the foraging ecology and division of labor in *M. barbarus* remains therefore to be investigated.

Competing interests
The authors declare no competing or financial interests.

Supplementary information
Supplementary information available online at
http://jeb.biologists.org/lookup/doi/10.1242/jeb.205690.supplemental

References
Alexander, R. M. (2003). *Principles of Animal Locomotion*. Princeton, NJ: Princeton University Press.

Bartholomew, G. A., Lighton, J. R. B. and Feener, D. H. (1988). Energetics of trail running, load carriage, and emigration in the column-raiding army ant *Eciton hamatum*. *Physiol. Zool.* **61**, 57-68. doi:10.1086/physzool.61.1.30163737

Bartsch, M. S., Federle, W., Full, R. J. and Kenny, T. W. (2007). A multiaxis force sensor for the study of insect biomechanics. *J. Microelectromech. Syst.* **16**, 709-718. doi:10.1109/JMEMS.2007.893677

Batschelet, E. (1981). *Circular Statistics in Biology*. London: Academic Press.

Bender, J. A., Simpson, E. M., Tietz, B. R., Daltorio, K. A., Quinn, R. D. and Ritzmann, R. E. (2011). Kinematic and behavioral evidence for a distinction between trotting and ambling gaits in the cockroach *Blaberus discoidalis*. *J. Exp. Biol.* **214**, 2057-2064. doi:10.1242/jeb.056481

Bernadou, A., Felden, A., Moreau, M., Moretto, P. and Fourcassié, V. (2016). Ergonomics of load transport in the seed harvesting ant *Messor barbarus*: morphology influences transportation method and efficiency. *J. Exp. Biol.* **219**, 2920-2927. doi:10.1242/jeb.141556

Bonner, J. T. (2006). *Why Size Matters: from Bacteria to Blue Whales*. Princeton, NJ: Princeton University Press.

Burd, M. (2000). Body size effects on locomotion and load carriage in the highly polymorphic leaf-cutting ants *Atta colombica* and *Atta cephalotes*. *Behav. Ecol.* **11**, 125-131. doi:10.1093/beheco/11.2.125

Cerdan, F. (1989). Etude de la biologie, de l'écologie et du comportement des fourmis moissonneuses du genre Messor (Hymenoptera, Formicidae). *PhD thesis*, Université de Provence, Marseille, France.

Czaczkes, T. J. and Ratnieks, F. L. W. (2013). Cooperative transport in ants (*Hymenoptera: Formicidae*) and elsewhere. *Myrmecolog. News* **18**, 1-11.

Davidson, D. W. (1978). Size variability in the worker caste of a social insect (*Veromessor pergandei* Mayr) as a function of the competitive environment. *Am. Nat.* **112**, 523-532. doi:10.1086/283294

Delcomyn, F. (1981). Insect locomotion on land. In *Locomotion and Energetics in Arthropods* (ed. C. F. Herreid and C. R. Fourtner), pp. 103-125. New York: Springer.

Dial, K. P., Greene, E. and Irschick, D. J. (2008). Allometry of behavior. *Trends in Ecol. Evol.* **23**, 394-401. doi:10.1016/j.tree.2008.03.005

Endlein, T. and Federle, W. (2008). Walking on smooth or rough ground: passive control of pretarsal attachment in ants. *J. Comp. Physiol. A* **194**, 49-60. doi:10.1007/s00359-007-0287-x

Endlein, T. and Federle, W. (2015). On heels and toes: How ants climb with adhesive pads and tarsal friction hair arrays. *PLoS ONE* **10**, 1-16. doi:10.1371/journal.pone.0141269

Federle, W., Brainerd, E. L., McMahon, T. A. and Holldobler, B. (2001). Biomechanics of the movable pretarsal adhesive organ in ants and bees. *Proc. Natl. Acad. Sci. USA* **98**, 6215-6220. doi:10.1073/pnas.111139298

Felden, A. (2014). Biomechanics of load-carriage in the seed-harvester ant *Messor barbarus*. *Masters thesis*. Université Paul Sabatier, Toulouse, France.

Fleming, P. A. and Bateman, P. W. (2007). Just drop it and run: the effect of limb autotomy on running distance and locomotion energetics of field crickets (*Gryllus bimaculatus*). *J. Exp. Biol.* **210**, 1446-1454. doi:10.1242/jeb.02757

Grabowska, M., Godlewska, E., Schmidt, J. and Daun-Gruhn, S. (2012). Quadrupedal gaits in hexapod animals - inter-leg coordination in free-walking adult stick insects. *J. Exp. Biol.* **215**, 4255-4266. doi:10.1242/jeb.073643

Gravish, N., Monaenkova, D., Goodisman, M. A. D. and Goldman, D. I. (2013). Climbing, falling, and jamming during ant locomotion in confined environments. *Proc. Natl. Acad. Sci. USA* **110**, 9746-9751. doi:10.1073/pnas.1302428110

Heredia, A. and Detrain, C. (2000). Worker size polymorphism and ethological role of sting associated glands in the harvester ant *Messor barbarus*. *Insectes Soc.* **47**, 383-389. doi:10.1007/PL00001735

Hölldobler, B. and Wilson, E. O. (1990). *The Ants*. Cambridge: The Bleknap Press of the Harvard University Press.

Hughes, G. M. (1952). The co-ordination of insect movements. *J. Exp. Biol.* **29**, 267-285.

Jagnandan, K. and Higham, T. E. (2018). How rapid changes in body mass affect the locomotion of terrestrial vertebrates: Ecology, evolution and biomechanics of a natural perturbation. *Biol. J. Linnean Soc.* **124**, 279-293. doi:10.1093/biolinnean/bly056

Koditschek, D. E., Full, R. J. and Buehler, M. (2004). Mechanical aspects of legged locomotion control. *Arthropod. Struct. Dev.* **33**, 251-272. doi:10.1016/j.asd.2004.06.003

Lagos, P. A. (2017). A review of escape behaviour in orthopterans. *J. Zool.* **303**, 165-177. doi:10.1111/jzo.12496

Lighton, J. R. B., Bartholomew, G. A. and Feener, D. H. (1987). Energetics of locomotion and load carriage and a model of the energy cost of foraging in the leaf-cutting ant *Atta colombica* guer. *Physiol. Zool.* **60**, 524-537. doi:10.1086/physzool.60.5.30156127

Mendes, C. S., Bartos, I., Akay, T., Márka, S. and Mann, R. S. (2013). Quantification of gait parameters in freely walking wild type and sensory deprived *Drosophila melanogaster*. *eLife* **2**, e00565. doi:10.7554/eLife.00565

Moll, K., Roces, F. and Federle, W. (2010). Foraging grass-cutting ants (*Atta vollenweideri*) maintain stability by balancing their loads with controlled head movements. *J. Comp. Physiol.* **196**, 471-480. doi:10.1007/s00359-010-0535-3

Moll, K., Roces, F. and Federle, W. (2013). How load-carrying ants avoid falling over: mechanical stability during foraging in *Atta vollenweideri* grass-cutting ants. *PLoS ONE* **8**, e52816. doi:10.1371/journal.pone.0052816

Pfeffer, S. E., Wahl, V. L. and Wittlinger, M. (2016). How to find home backwards? Locomotion and inter-leg coordination during rearward walking of *Cataglyphis fortis* desert ants. *J. Exp. Biol.* **219**, 2110-2118. doi:10.1242/jeb.137778

Ramdya, P., Thandiackal, R., Cherney, R., Asselborn, T., Benton, R., Ijspeert, A. J. and Floreano, D. (2017). Climbing favours the tripod gait over alternative faster insect gaits. *Nat. Commun.* **8**, 14494. doi:10.1038/ncomms14494

Reinhardt, L. and Blickhan, R. (2014a). Level locomotion in wood ants: evidence for grounded running. *J. Exp. Biol.* **217**, 2358-2370. doi:10.1242/jeb.098426

Reinhardt, L. and Blickhan, R. (2014b). Ultra-miniature force plate for measuring triaxial forces in the micronewton range. *J. Exp. Biol.* **217**, 704-710. doi:10.1242/jeb.094177

Reinhardt, L., Weihmann, T. and Blickhan, R. (2009). Dynamics and kinematics of ant locomotion: do wood ants climb on level surfaces? *J. Exp. Biol.* **212**, 2426-2435. doi:10.1242/jeb.026880

Rissing, S. W. (1982). Foraging velocity of seed-harvester ants, *Veromessor pergandei* (Hymenoptera: Formicidae). *Environ. Entmol.* **11**, 905-907. doi:10.1093/ee/11.4.905

Röschard, J. and Roces, F. (2002). The effect of load length, width and mass on transport rate in the grass-cutting ant *Atta vollenweideri*. *Oecologia* **131**, 319-324. doi:10.1007/s00442-002-0882-z

Schmidt-Nielsen, K. (1984). *Scaling: Why is Animal Size so Important?* Cambridge, UK: Cambridge University Press.

Segre, P. S. and Taylor, E. D. (2019). Large ants do not carry their fair share: maximal load-carrying performance of leaf-cutter ants (*Atta cephalotes*). *J. Exp. Biol.* **222**, 1-4. doi:10.1242/jeb.199240

Seidl, T. and Wehner, R. (2008). Walking on inclines: How do desert ants monitor slope and step length? *Front. Zool.* **5**, 1-15. doi:10.1186/1742-9994-5-8

Spence, A. J., Revzen, S., Seipel, J., Mullens, C. and Full, R. J. (2010). Insects running on elastic surfaces. *J. Exp. Biol.* **213**, 1907-1920. doi:10.1242/jeb.042515

Ting, L. H., Blickhan, R. and Full, R. J. (1994). Dynamic and static stability in hexapedal runners. *J. Exp. Biol.* **197**, 251-269.

Wahl, V., Pfeffer, S. E. and Wittlinger, M. (2015). Walking and running in the desert ant *Cataglyphis fortis*. *J. Comp. Physiol. A* **201**, 645-656. doi:10.1007/s00359-015-0999-2

Watson, J. T., Ritzmann, R. E., Zill, S. N. and Pollack, A. J. (2002). Control of obstacle climbing in the cockroach, *Blaberus discoidalis*. I. Kinematics. *J. Comp. Physiol. A* **188**, 39-53. doi:10.1007/s00359-002-0277-y

Wöhrl, T., Reinhardt, L. and Blickhan, R. (2017). Propulsion in hexapod locomotion: how do desert ants traverse slopes? *J. Exp. Biol.* **220**, 1618-1625. doi:10.1242/jeb.137505

Wosnitza, A., Bockemuhl, T., Dubbert, M., Scholz, H. and Buschges, A. (2013). Inter-leg coordination in the control of walking speed in *Drosophila*. *J. Exp. Biol.* **216**, 480-491. doi:10.1242/jeb.078139

Zollikofer, C. P. E. (1994a). Stepping patterns in ants - Part I - influence of speed and curvature. *J. Exp. Biol.* **192**, 119-127.

Zollikofer, C. P. E. (1994b). Stepping patterns in ants - Part III - influence of load. *J. Exp. Biol.* **192**, 119-127.